Int. J. Solids Structures Vol. 16, pp. 361–373
Pergamon Press Ltd., 1980. Printed in Great Britain

ASYMMETRIC BENDING OF ANNULAR PLATES

J. T. TIELKING

Mechanical Engineering Department, Texas A&M University, College Station, TX 77843, U.S.A.

(*Received* 12 *January* 1979; *in revised form* 29 *May* 1979)

Abstract—An isotropic, variable thickness, annular plate with clamped edges is bent by prescribing a rotation of the inner edge about a diameter, with the outer edge held fixed. The potential energy formulation of von Karman plate theory and the Ritz method are employed to calculate solutions for deformation and stress. The external moment is obtained with Castigliano's theorem. Solutions are presented to show the effect of a large rotation on the bending and membrane stresses in the plate and to show how these stresses are affected by the thickness distribution.

INTRODUCTION

Annular plates of both uniform and variable thickness have many applications in engineering structures. An application that is currently receiving considerable attention is the use of a variable thickness annular plate in a coupling for power transmission shafts which may normally become misaligned, due to shaft flexure or thermal expansion during operation; the misalignment is accommodated by asymmetric bending of the plate. Such plates have been successfully designed to sustain transverse deflection cycles that are well into the nonlinear range of the load-deflection response. Control of the bending stresses may be achieved by design of the plate thickness profile. However, most coupling plates are currently designed with a "hyperbolic profile", in which the thickness varies as the inverse square of the radius; this profile is optimum only for torsional shear stress in the absence of flexure.

Small-deflection solutions for symmetric and asymmetric bending of annular plates, with certain thickness profiles, have been available for many years. Calculated data for plates with uniform thickness, and thickness that increases linearly with radius, are collected in a book by Timoshenko[1]; corrections and additional data for the case of moment loading of uniform thickness plates were recently given by Brock[2]. Design data for plates with thickness that decreases according to a power law are given in a comprehensive paper by Wolff[3]. These references describe closed form, or series, solutions of the classical equilibrium equations for a thin plate. The finite element method has been utilized for calculation of asymmetric bending solutions for small deflections of annular plates when the plate thickness is uniform[4] or changing linearly with radius[5].

A number of publications are found which describe solutions for large-deflection bending of annular plates. Most of these solutions, however, require the plate to be prestressed with a radial load [e.g. Refs. 6–8] and all except Ref. [9] treat only uniform thickness plates. Large-deflection solutions that do not presume prestress are given for symmetric bending by Hart and Evans[10] and for unsymmetrical bending by Alzheimer and Davis[11]. References[6–8, 10, 11] describe numerical solutions of geometrically nonlinear equilibrium equations for a plate of uniform thickness. Reference[9] utilizes von Karman plate theory and the Ritz method to calculate large-deflection solutions for symmetric bending of variable thickness annular plates.

The work reported in this paper extends the energy formulation and solution procedure utilized in [9] to include asymmetric bending of variable thickness annular plates. Boundary conditions for the special case of asymmetric bending treated by Alzheimer and Davis[11] are used and the solution obtained by the energy method is compared with experimental data given in [11]. Additional solutions are presented to show the effect of taper on the stress distributions in the same plate.

FORMULATION

The strain energy of the plate is separated into two components: membrane energy, U_m, produced by extensional strains, and bending energy, U_b, produced by curvature changes. For

asymmetric bending, these energy expressions are

$$U_m = \frac{1}{2}\int\int K\left[\epsilon_{rr}^2 + \epsilon_{\theta\theta}^2 + 2\nu\epsilon_{rr}\epsilon_{\theta\theta} + \frac{1}{2}(1-\nu)\epsilon_{r\theta}^2\right] r\,dr\,d\theta \tag{1}$$

$$U_b = \frac{1}{2}\int\int D[(\kappa_{rr}+\kappa_{\theta\theta})^2 - 2(1-\nu)(\kappa_{rr}\kappa_{\theta\theta} - \kappa_{r\theta}^2)]r\,dr\,d\theta \tag{2}$$

where

$$K = \frac{2Gt}{1-\nu} \quad \text{and} \quad D = \frac{Gt^3}{6(1-\nu)}$$

are the extensional and flexural rigidities, respectively, with G and ν denoting the shear modulus and Poisson's ratio. An axisymmetric thickness variation $t(r)$ is assumed; it influences the strain energy by remaining inside the integrals. The integrals are evaluated over the plate midsurface, in the region $(0 \le \theta \le 2\pi,\ r_b \le r \le r_a)$ where r_b and r_a are the inner and outer radii, respectively. If the plate is only edge loaded (assumed in this paper), the potential energy, Π, is

$$\Pi = U_m + U_b. \tag{3}$$

The following formulation for large-deflection bending is commonly known as the von Karman theory of flat plates[12]. The strain-displacement equations are

$$\begin{aligned}
\epsilon_{rr} &= \frac{\partial u}{\partial r} + \frac{1}{2}\left(\frac{\partial w}{\partial r}\right)^2 \\
\epsilon_{r\theta} &= \frac{1}{r}\frac{\partial u}{\partial \theta} + \frac{\partial v}{\partial r} - \frac{v}{r} + \left(\frac{\partial w}{\partial r}\right)\left(\frac{1}{r}\frac{\partial w}{\partial \theta}\right) \\
\epsilon_{\theta\theta} &= \frac{u}{r} + \frac{1}{r}\frac{\partial v}{\partial \theta} + \frac{1}{2}\left(\frac{1}{r}\frac{\partial w}{\partial \theta}\right)^2
\end{aligned} \tag{4}$$

and the curvatures of the deformed midsurface are given by

$$\begin{aligned}
\kappa_{rr} &= \frac{\partial^2 w}{\partial r^2} \\
\kappa_{r\theta} &= \frac{1}{r}\left(\frac{\partial^2 w}{\partial r\partial\theta} - \frac{1}{r}\frac{\partial w}{\partial \theta}\right) \\
\kappa_{\theta\theta} &= \frac{1}{r}\left(\frac{1}{r}\frac{\partial^2 w}{\partial \theta^2} + \frac{\partial w}{\partial r}\right).
\end{aligned} \tag{5}$$

In the above, $u(r, \theta)$ and $v(r, \theta)$ are tangential displacements in the radial and circumferential directions, respectively, and $w(r, \theta)$ is the transverse displacement of a point initially on the undeformed mid-surface of the plate. The stress and moment resultants are

$$\begin{aligned}
N_{rr} &= K(\epsilon_{rr} + \nu\epsilon_{\theta\theta}) \\
N_{r\theta} &= Gt\epsilon_{r\theta} \\
N_{\theta\theta} &= K(\epsilon_{\theta\theta} + \nu\epsilon_{rr})
\end{aligned} \tag{6}$$

$$\begin{aligned}
M_{rr} &= -D(\kappa_{rr} + \nu\kappa_{\theta\theta}) \\
M_{r\theta} &= D(1-\nu)\kappa_{r\theta} \\
M_{\theta\theta} &= -D(\kappa_{\theta\theta} + \nu\kappa_{rr}).
\end{aligned} \tag{7}$$

The sign convention for the displacements and the resultants is given in Fig. 1. The moment-

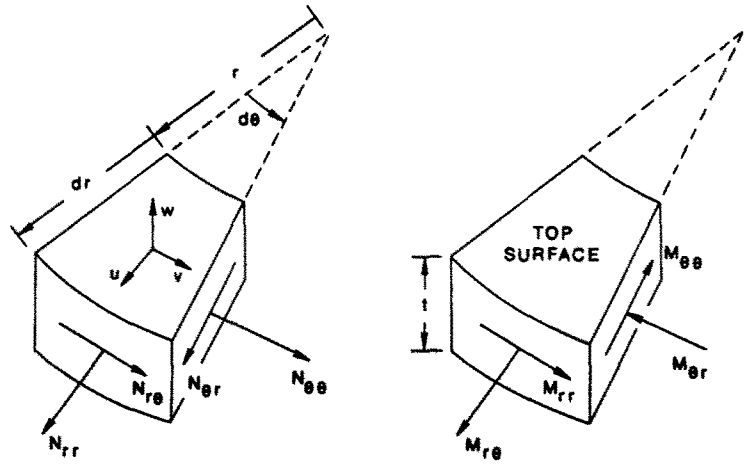

Fig. 1. Positive directions of displacements, stress resultants, and moment resultants.

curvature expressions are written so that a positive bending moment, M_{rr} or $M_{\theta\theta}$, will make the top surface convex. A positive twist moment, $M_{r\theta}$, will produce positive slopes $(\partial w/\partial r)$ and $(\partial w/\partial\theta)$.

For the example solutions, the plate edges are rigidly clamped and bending is produced by prescribing a rotation, α, of the inner edge (called the hub) about a diameter, while the outer edge (called the rim) is held fixed.† The displacement solution functions are therefore required to satisfy the following forced boundary conditions, which describe built-in edges.

Inner Edge

$$\begin{aligned} u(r_b, \theta) &= r_b(\cos\alpha - 1)\cos^2\theta \\ v(r_b, \theta) &= r_b(1 - \cos\alpha)\sin\theta\cos\theta \\ w(r_b, \theta) &= r_b \sin\alpha\cos\theta \\ \frac{\partial w}{\partial r}(r_b, \theta) &= \sin\alpha\cos\theta \end{aligned} \tag{8}$$

Outer Edge

$$\begin{aligned} u(r_a, \theta) &= 0 \\ v(r_a, \theta) &= 0 \\ w(r_a, \theta) &= 0 \\ \frac{\partial w}{\partial r}(r_a, \theta) &= 0 \end{aligned} \tag{9}$$

The boundary conditions expressed by eqns (8) and (9) imply the bending is symmetric about the hub diameter that is perpendicular to the hub rotation axis. The diameter of symmetry is located at $\theta = 0$ and the potential energy is integrated over the plate half in the region $(0 \le \theta \le \pi,\ r_b \le r \le r_a)$. The displacements $u(r, \theta)$ and $w(r, \theta)$ will be symmetric about $\theta = 0,\ \pi$ and the displacement $v(r, \theta)$ will be antisymmetric about $\theta = 0,\ \pi$. Further, the plate diameter coinciding with the hub rotation axis will remain undeformed; this imposes the following additional conditions on the displacement solution.

$$\begin{aligned} u(r, \pi/2) &= u(r, 3\pi/2) = 0 \\ v(r, \pi/2) &= v(r, 3\pi/2) = 0 \\ w(r, \pi/2) &= w(r, 3\pi/2) = 0. \end{aligned}$$

†This particular case of asymmetric bending has been termed skew bending[3].

Regardless of the nature of the bending, the expression $(\kappa_{rr}\kappa_{\theta\theta} - \kappa_{r\theta}^2)$, appearing in eqn (2), contributes nothing to the differential equations of the plate. It may, however, contribute to the natural boundary conditions[12]. Since the specific plate problem solved in this paper is formulated without natural boundary conditions, the expression has been dropped from eqn (2) and the bending energy calculated according to the simpler expression

$$U_b = \frac{1}{2}\int\int D(\kappa_{rr} + \kappa_{\theta\theta})^2 r \, dr \, d\theta. \tag{10}$$

NUMERICAL SOLUTION

The solution is obtained by application of the principle of minimum potential energy which states that, of all geometrically admissible displacement solutions, the exact solution minimizes the potential energy, Π. A displacement solution is geometrically admissible if it satisfies the forced boundary conditions given by eqns (8) and (9). In most nonlinear problems only an approximate solution can be found by using, e.g. the Ritz method[12] which is employed here.

Ritz method

To apply the Ritz method, approximate solutions for the displacement functions are written as two-dimensional finite series.

$$\begin{aligned} u(r,\theta) &= u_0(r,\theta) + \sum_{i=1}^{M}\sum_{j=1}^{N} a_{ij}u^{ij}(r,\theta) \\ v(r,\theta) &= v_0(r,\theta) + \sum_{i=1}^{M}\sum_{j=1}^{N} b_{ij}v^{ij}(r,\theta) \\ w(r,\theta) &= w_0(r,\theta) + \sum_{i=1}^{M}\sum_{j=1}^{N} c_{ij}w^{ij}(r,\theta) \end{aligned} \tag{11}$$

where the functions u_0, v_0, w_0 satisfy the boundary conditions (8) and (9), and will be called initial functions. The function u^{ij}, v^{ij}, w^{ij} all satisfy homogeneous forced boundary conditions; they are frequently called coordinate functions. With an infinite number of terms, these series will converge to the exact solution provided each sequence of coordinate functions is complete in the integration interval. Although these displacement functions will stabilize in a reasonable number of terms, the bending stresses (which require the second derivative of w) may not be acceptable† unless a large number of terms are taken, thereby introducing other numerical difficulties. In the present work, convergence is enhanced and acceptable bending stresses are found by utilizing displacement solution functions that are capable of satisfying natural boundary conditions, in addition to being geometrically admissible. This capability is acquired if the second and third derivatives of w_0 and w^{ij}, with respect to r, do not vanish on the boundaries.

Solution functions

The initial functions employed here are

$$\begin{aligned} u_0(r,\theta) &= r_b(\cos\alpha - 1)\left(\frac{r_a - r}{r_a - r_b}\right)\cos^2\theta \\ v_0(r,\theta) &= r_b(1 - \cos\alpha)\left(\frac{r_a - r}{r_a - r_b}\right)\sin\theta\cos\theta \end{aligned} \tag{12}$$

$$\begin{aligned} w_0(r,\theta) = {} & [2r^3 - 3(r_a + r_b)r^2 + 6r_a r_b r + r_a^2(r_a - 3r_b)]\frac{\Delta(\theta)}{(r_a - r_b)^3} \\ & + [r^3 - (2r_a + r_b)r^2 + r_a(r_a + 2r_b)r - r_a^2 r_b]\frac{\Phi(\theta)}{(r_a - r_b)^2} \end{aligned} \tag{13}$$

†This is perhaps the main reason that the principle of minimum potential energy is not often employed for stress analysis.

where

$$\Delta(\theta) = r_b \sin\alpha \cos\theta \qquad \text{and} \qquad \Phi(\theta) = \sin\alpha \cos\theta$$

are the deflection and slope of the rotated hub circumference. Equation (13) is the exact small-deflection solution for a beam with clamped ends, when the left end is deflected as shown in Fig. 2.

The coordinate functions employed are

$$\begin{aligned} u^{ij}(r,\theta) &= u^i(r)\cos(2j-1)\theta \\ v^{ij}(r,\theta) &= u^i(r)\sin 2j\theta \\ w^{ij}(r,\theta) &= w^i(r)\cos(2j-1)\theta \end{aligned} \tag{14}$$

where $u^i(r)$ and $w^i(r)$ are given by

$$u^i(r) = \sin i\pi\left(\frac{r_a - r}{r_a - r_b}\right) \tag{15}$$

$$\begin{aligned} w^i(r) = {} & \cosh\lambda_i\left(\frac{r_a - r}{r_a - r_b}\right) - \cos\lambda_i\left(\frac{r_a - r}{r_a - r_b}\right) \\ & - \left(\frac{\cosh\lambda_i - \cos\lambda_i}{\sinh\lambda_i - \sin\lambda_i}\right)\left[\sinh\lambda_i\left(\frac{r_a - r}{r_a - r_b}\right) - \sin\lambda_i\left(\frac{r_a - r}{r_a - r_b}\right)\right]. \end{aligned} \tag{16}$$

The functions $w^i(r)$ are the natural vibration modes of a beam with clamped ends. The λ_i are the natural frequencies, obtained from the frequency equation

$$\cos\lambda \cosh\lambda = 1. \tag{17}$$

Values of λ_i are tabulated in most vibration handbooks. For this analysis, they were taken from Ref. [13]. The solution functions defined by eqns (11)–(16) satisfy the forced boundary conditions expressed by eqns (8) and (9) and the symmetry conditions. They also possess the natural boundary condition capability discussed above.

The solution functions are used to calculate the strains and curvatures which appear in the extensional strain energy expression (1) and the bending strain energy expression (10). The specific functions permit the energy expressions to be integrated. The potential energy, Π given by eqn (3), is then reduced to an algebraic function of the $3 \times M \times N$ constants a_{ij}, b_{ij}, c_{ij}, that are needed for the summations in eqns (11).

$$\Pi = \Pi(a_{ij}; b_{ij}; c_{ij}).$$

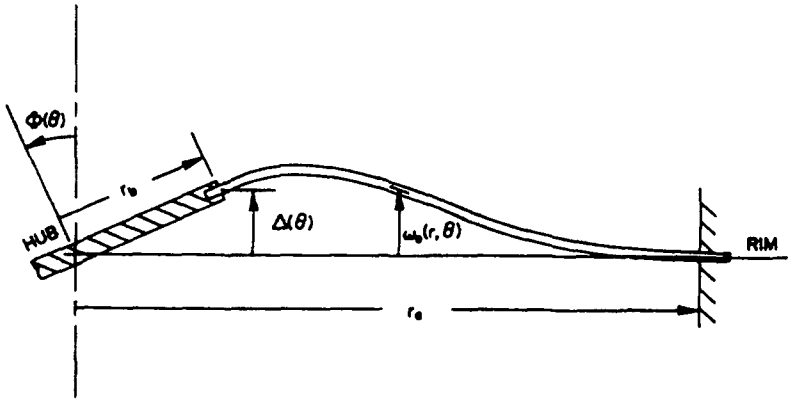

Fig. 2. Deflected beam used for the initial shape in the solution of an asymmetric plate bending problem.

The energy minimizing constants are found by solving the following $3 \times M \times N$ algebraic equations.

$$\begin{aligned} \frac{\partial \Pi}{\partial a_{ij}} &= \frac{\partial U_m}{\partial a_{ij}} + \frac{\partial U_b}{\partial a_{ij}} = 0 \\ \frac{\partial \Pi}{\partial b_{ij}} &= \frac{\partial U_m}{\partial b_{ij}} + \frac{\partial U_b}{\partial b_{ij}} = 0 \\ \frac{\partial \Pi}{\partial c_{ij}} &= \frac{\partial U_m}{\partial c_{ij}} + \frac{\partial U_b}{\partial c_{ij}} = 0 \end{aligned} \qquad \begin{aligned} &i = 1, 2, \ldots, M \\ &j = 1, 2, \ldots, N \end{aligned} \tag{18}$$

where

$$\begin{aligned} \frac{\partial U_m}{\partial a_{ij}} &= \int\int [rN_{rr}u^{ij}_{,r} + N_{\theta\theta}u^{ij} + N_{r\theta}u^{ij}_{,\theta}]\,dr\,d\theta \\ \frac{\partial U_b}{\partial a_{ij}} &= 0 \\ \frac{\partial U_m}{\partial b_{ij}} &= \int\int [N_{\theta\theta}v^{ij}_{,\theta} + N_{r\theta}(rv^{ij}_{,r} - v^{ij})]\,dr\,d\theta \\ \frac{\partial U_b}{\partial b_{ij}} &= 0 \\ \frac{\partial U_m}{\partial c_{ij}} &= \int\int \left[rN_{rr}w_{,r}w^{ij}_{,r} + \frac{1}{r}N_{\theta\theta}w_{,\theta}w^{ij}_{,\theta} + N_{r\theta}(w_{,r}w^{ij}_{,\theta} + w^{ij}_{,r}w_{,\theta})\right] dr\,d\theta \\ \frac{\partial U_b}{\partial c_{ij}} &= \int\int Dr(\kappa_{rr} + \kappa_{\theta\theta})\left(\frac{\partial \kappa_{rr}}{\partial c_{ij}} + \frac{\partial \kappa_{\theta\theta}}{\partial c_{ij}}\right) dr\,d\theta. \end{aligned} \tag{19}$$

A plate solution begins by assuming that all of the coefficients a_{ij}, b_{ij} and c_{ij} are zero. Successive corrections to these coefficients are obtained by iterative solutions of the Newton–Raphson matrix equation,

$$\begin{aligned} \sum_{k=1}^{M}\sum_{l=1}^{N}\frac{\partial^2\Pi}{\partial a_{kl}\partial a_{ij}}\Delta a_{kl} + \sum_{k=1}^{M}\sum_{l=1}^{N}\frac{\partial^2\Pi}{\partial b_{kl}\partial a_{ij}}\Delta b_{kl} + \sum_{k=1}^{M}\sum_{l=1}^{N}\frac{\partial^2\Pi}{\partial c_{kl}\partial a_{ij}}\Delta c_{kl} &= \frac{\partial\Pi}{\partial a_{ij}} \\ \sum_{k=1}^{M}\sum_{l=1}^{N}\frac{\partial^2\Pi}{\partial a_{kl}\partial b_{ij}}\Delta a_{kl} + \sum_{k=1}^{M}\sum_{l=1}^{N}\frac{\partial^2\Pi}{\partial b_{kl}\partial b_{ij}}\Delta b_{kl} + \sum_{k=1}^{M}\sum_{l=1}^{N}\frac{\partial^2\Pi}{\partial c_{kl}\partial b_{ij}}\Delta c_{kl} &= \frac{\partial\Pi}{\partial b_{ij}} \\ \sum_{k=1}^{M}\sum_{l=1}^{N}\frac{\partial^2\Pi}{\partial a_{kl}\partial c_{ij}}\Delta a_{kl} + \sum_{k=1}^{M}\sum_{l=1}^{N}\frac{\partial^2\Pi}{\partial b_{kl}\partial c_{ij}}\Delta b_{kl} + \sum_{k=1}^{M}\sum_{l=1}^{N}\frac{\partial^2\Pi}{\partial c_{kl}\partial c_{ij}}\Delta c_{kl} &= \frac{\partial\Pi}{\partial c_{ij}}. \end{aligned} \tag{20}$$

This equation is symmetric. The corrected coefficients, after iteration n, are

$$\begin{aligned} a^{n+1}_{ij} &= a^{n}_{ij} - \Delta a_{ij} \\ b^{n+1}_{ij} &= b^{n}_{ij} - \Delta b_{ij} \\ c^{n+1}_{ij} &= c^{n}_{ij} - \Delta c_{ij}. \end{aligned} \qquad \begin{aligned} &i = 1, 2, \ldots, M \\ &j = 1, 2, \ldots, N \end{aligned} \tag{21}$$

The starting coefficients are $a^{0}_{ij} = b^{0}_{ij} = c^{0}_{ij} = 0$. The iterations continue until the corrections have negligible effect on the displacements computed from eqns (11).

The Newton–Raphson iteration for the minimizing coefficients requires the second derivatives of the strain energies, which are recorded below in the form used by the computer program. Only the derivatives appearing in the upper triangle of eqn (20) are needed.

$$\frac{\partial^2 U_m}{\partial a_{kl}\partial a_{ij}} = \int\int \left[r\frac{\partial N_{rr}}{\partial a_{kl}} u^{ij}_{,r} + \frac{\partial N_{\theta\theta}}{\partial a_{kl}} u^{ij} + \frac{\partial N_{r\theta}}{\partial a_{kl}} u^{ij}_{,\theta} \right] dr\, d\theta$$

$$\frac{\partial^2 U_m}{\partial b_{kl}\partial a_{ij}} = \int\int \left[r\frac{\partial N_{rr}}{\partial b_{kl}} u^{ij}_{,r} + \frac{\partial N_{\theta\theta}}{\partial b_{kl}} u^{ij} + \frac{\partial N_{r\theta}}{\partial b_{kl}} u^{ij}_{,\theta} \right] dr\, d\theta$$

$$\frac{\partial^2 U_m}{\partial c_{kl}\partial a_{ij}} = \int\int \left[r\frac{\partial N_{rr}}{\partial c_{kl}} u^{ij}_{,r} + \frac{\partial N_{\theta\theta}}{\partial c_{kl}} u^{ij} + \frac{\partial N_{r\theta}}{\partial c_{kl}} u^{ij}_{,\theta} \right] dr\, d\theta$$

$$\frac{\partial^2 U_m}{\partial b_{kl}\partial b_{ij}} = \int\int \left[\frac{\partial N_{\theta\theta}}{\partial b_{kl}} v^{ij}_{,\theta} + \frac{\partial N_{r\theta}}{\partial b_{kl}} (rv^{ij}_{,r} - v^{ij}) \right] dr\, d\theta \tag{22}$$

$$\frac{\partial^2 U_m}{\partial c_{kl}\partial b_{ij}} = \int\int \left[\frac{\partial N_{\theta\theta}}{\partial c_{kl}} v^{ij}_{,\theta} + \frac{\partial N_{r\theta}}{\partial c_{kl}} (rv^{ij}_{,r} - v^{ij}) \right] dr\, d\theta$$

$$\frac{\partial^2 U_m}{\partial c_{kl}\partial c_{ij}} = \int\int \left[r\left(\frac{\partial N_{rr}}{\partial c_{kl}} w_{,r} + N_{rr} w^{kl}_{,r}\right) w^{ij}_{,r} + \frac{1}{r}\left(\frac{\partial N_{\theta\theta}}{\partial c_{kl}} w_{,\theta} + N_{\theta\theta} w^{kl}_{,\theta}\right) w^{ij}_{,\theta} \right.$$
$$\left. + \left(\frac{\partial N_{r\theta}}{\partial c_{kl}} w_{,r} + N_{r\theta} w^{kl}_{,r}\right) w^{ij}_{,\theta} + \left(\frac{\partial N_{r\theta}}{\partial c_{kl}} w_{,\theta} + N_{r\theta} w^{kl}_{,\theta}\right) w^{ij}_{,r} \right] dr\, d\theta$$

$$\frac{\partial^2 U_b}{\partial c_{kl}\partial c_{ij}} = \int\int Dr\left(\frac{\partial \kappa_{rr}}{\partial c_{kl}} + \frac{\partial \kappa_{\theta\theta}}{\partial c_{kl}}\right)\left(\frac{\partial \kappa_{rr}}{\partial c_{ij}} + \frac{\partial \kappa_{\theta\theta}}{\partial c_{ij}}\right) dr\, d\theta$$

External moment

After the energy minimizing coefficients have been determined to a reasonable degree of accuracy, the potential energy, Π, is evaluated. Castigliano's first theorem[14] is then used to calculate the external moment, M, needed to produce the prescribed hub rotation, α. Since the plate is only edge loaded, the potential energy is equal to the strain energy and the moment is given by

$$M = \frac{\partial \Pi}{\partial \alpha} \tag{23}$$

With large rotations, this energy derivative is obtained graphically. With small rotations, the potential energy is known to be a quadratic function of α, viz.

$$\Pi = \frac{1}{2} K_s \alpha^2 \tag{24}$$

where K_s is the rotational spring constant. In this case

$$K_s = 2\Pi/\alpha^2 \tag{25}$$

and

$$M = K_s\alpha = 2\Pi/\alpha. \tag{26}$$

The spring constant and external moment calculated from the potential energy by eqns (25) and (26) for small rotations are very accurate, as shown by comparison with known solutions [e.g. 1]. With large rotations, the strain energy is no longer a quadratic function of α but the Castigliano theorem remains valid and eqn (23) may still be used for calculating the external moment.

Stresses

The membrane, σ_N, and maximum-bending, σ_M, stresses shown in the next section are calculated according to the formulae

$$\sigma_N = N/t \quad \text{and} \quad \sigma_M = 6M/t^2 \tag{27}$$

where N and M take consistant subscripts rr, $\theta\theta$ or $r\theta$. The maximum stress distribution is in the radial direction and given by

$$\sigma_{rr} = \sigma_{N_{rr}} + \sigma_{M_{rr}}. \tag{28}$$

The maximum stress (radial) occurs on the diameter of deformation symmetry, at the hub for uniform thickness plates. It is shown in the calculated results that a variable thickness profile can shift the maximum stress to the rim.

CALCULATED RESULTS

All of the calculated results were obtained for an aluminum plate with Young's modulus $E = 10^7$ psi (68.95 GN/m^2) and Poisson's ratio $\nu = 0.33$. The hub and rim radii are $r_b = 3.6$ in (91.44 mm) and $r_a = 9.0$ in (228.6 mm). Fourteen terms ($M = 7$, $N = 2$) were taken for the displacement functions represented by eqns (11).

Uniform thickness

The plate described above, with uniform thickness $t = 0.0634$ in (1.61 mm), was analytically (using von Karman plate theory) and experimentally studied by Alzheimer and Davis[11, 15]. Experimental data from [11] are plotted in Fig. 3 to compare with the energy solution obtained by the procedure described in this paper. Although there is a consistant underprediction, the energy solution agrees fairly well with the experimental data points. It also coincides with the iterative solution of Alzheimer and Davis[11] up to approximately $\alpha = 1.5$ deg, where the iterative solution (not shown) begins to overpredict the nonlinear effect.

The effect of large rotation angles on the bending and membrane stresses in the radial direction, calculated according to eqns (27), is seen in Figs. 4 and 5. As one may expect, the bending stresses become very high at the edges of the plate; their behavior has been investigated as a boundary layer effect in large axisymmetric bending of annular plates[10]. To the writer's knowledge, the fluctuation of the corresponding membrane stress seen in Fig. 5 has not been previously computed. The iterative solution of Alzheimer and Davis shows a linear variation in the membrane stress for $\alpha = 1.5$ deg (see Fig. 6 of [15] for membrane and bending stress distributions). However, their solution is the result of the first iteration, beginning with zero membrane stress and the bending stress from linear theory. Additional iterations may be necessary to fully develop the membrane stress distribution. Note that the minima in the membrane stress distributions of Fig. 5 appear in the high curvature regions of the deflected plate. The midsurface deflections are indicated by the deflected radii shown in Fig. 6.

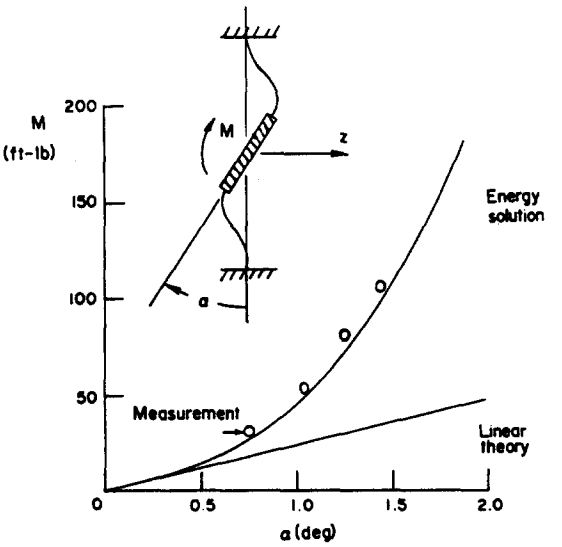

Fig. 3. Calculated and measured moment-rotation data.

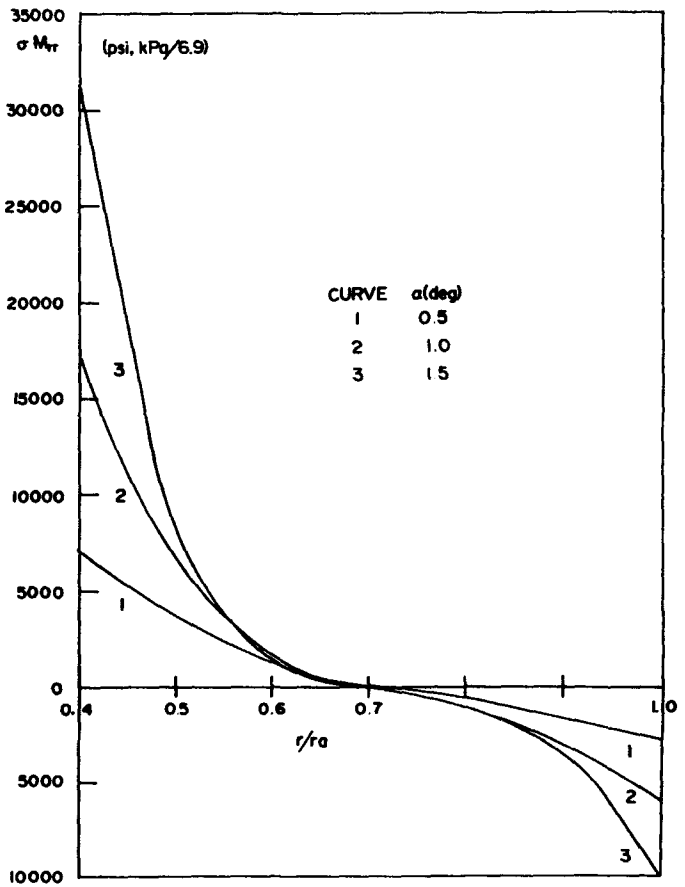

Fig. 4. Bending stress in the radial direction along the radius at $\theta = 0$.

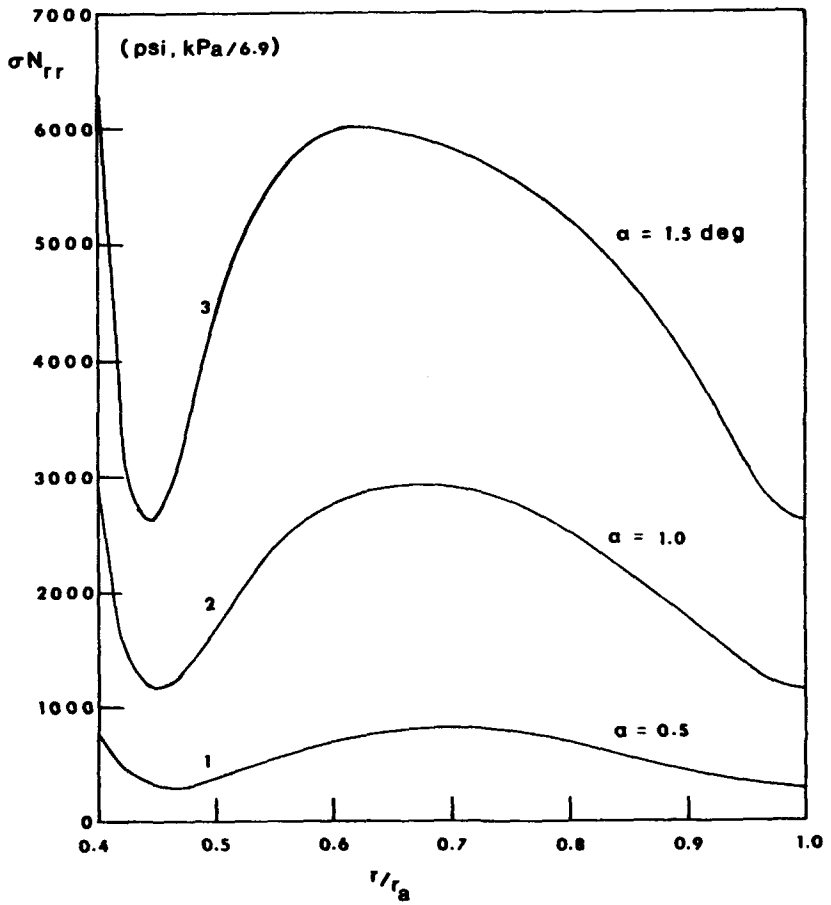

Fig. 5. Membrane stress in the radial direction along the radius at $\theta = 0$.

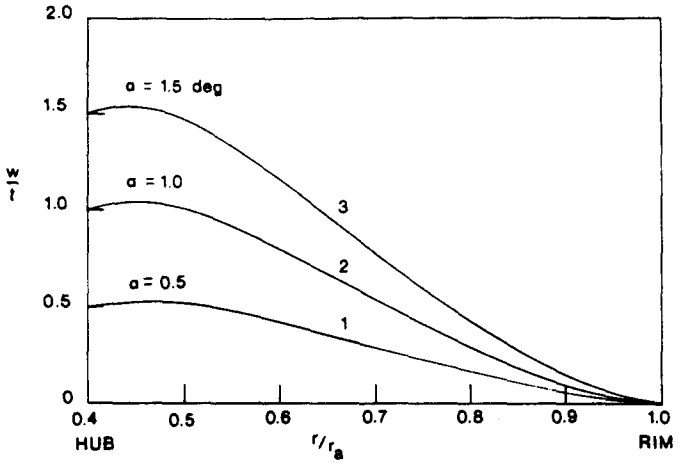

Fig. 6. Transverse deflection of the radius at $\theta = 0$.

Variable thickness

The effect of variable thickness is calculated here for plates tapered according to the thickness distribution function

$$t(r) = t_b\left(\frac{r}{r_b}\right)^{\beta} \tag{29}$$

where t_b is the thickness at the hub. The calculated results shown in Figs. 7–9 were all made with $t_b = 0.2$ in (5.08 mm).

The influence of an outward taper on the bending stress distribution is shown in Fig. 7. The hub rotation angle $\alpha = 0.05$ deg produces deformation in the linear range of the plates whose bending stresses are compared in Fig. 7. The taper exponent $\beta = -2$ produces the hyperbolic profile that is used in the coupling plate application mentioned in the Introduction.

Figures 8 and 9 show the effect of a large rotation angle on the bending and membrane stresses in the plate with the hyperbolic profile. This profile produces a membrane stress distribution (Fig. 9) that is considerably different from the membrane stress distribution in the uniform thickness plate (see Fig. 5). In spite of the wide fluctuation of the membrane stress, the

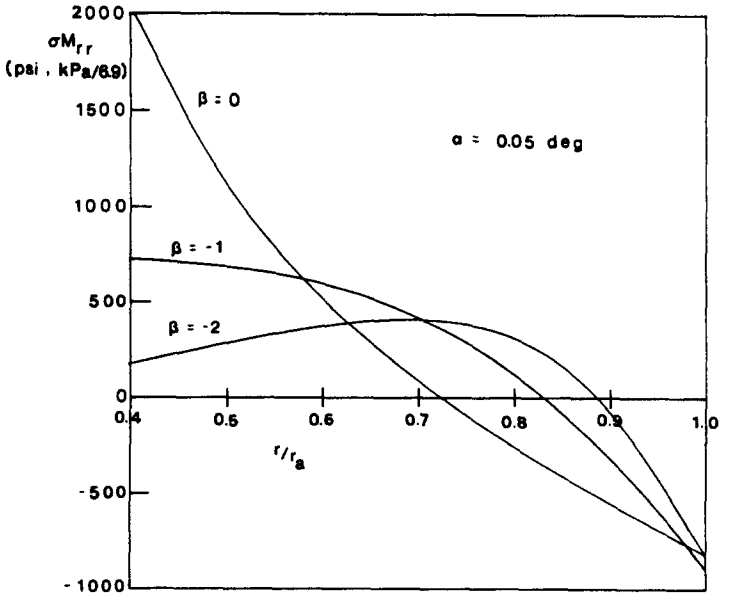

Fig. 7. Influence of outward taper on bending stress. Taper exponents: $\beta = 0$ (uniform thickness), $\beta = -1$, and $\beta = -2$ (hyperbolic taper).

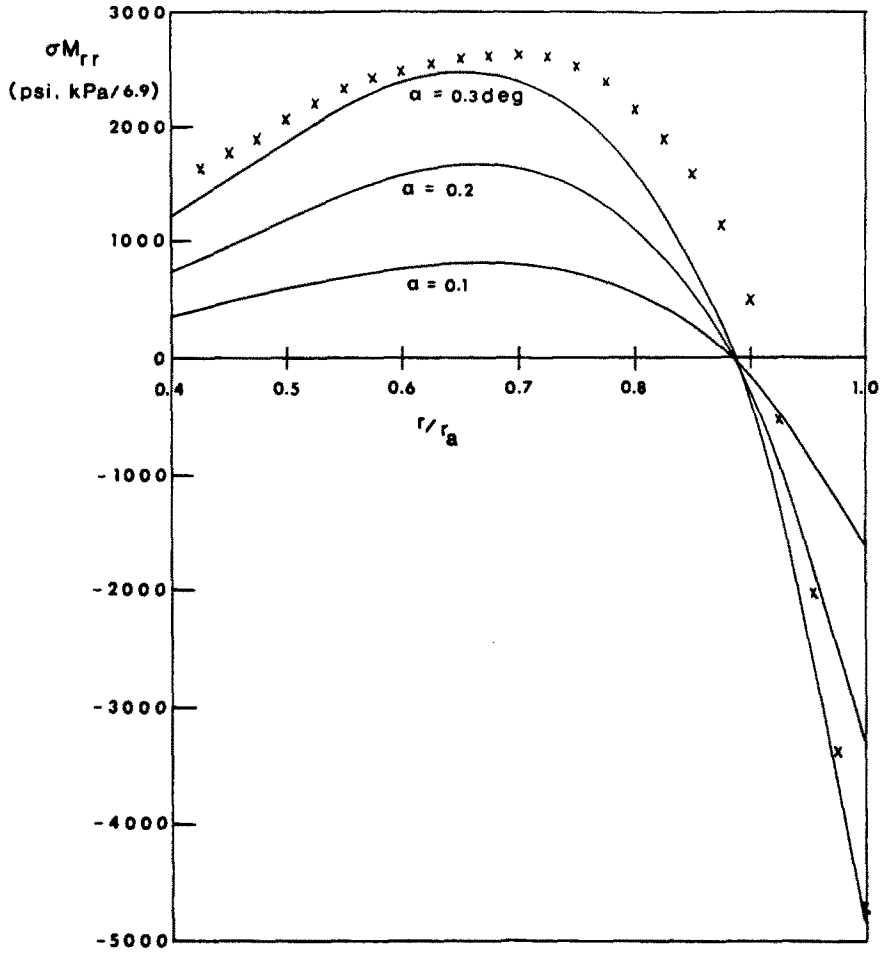

Fig. 8. Influence of a large hub rotation on the bending stress in a plate with hyperbolic taper. Discrete points show the surface stress σ_{rr} at $\alpha = 0.3$ deg.

general character of the maximum stress, calculated according to eqn (28), follows that of the bending stress. This is seen in Fig. 8 where the discrete points show the surface stress σ_{rr} for $\alpha = 0.3$ deg.

DISCUSSION

The deformation and stress solutions presented in this paper are derived from von Karman plate theory but the computational procedure could be applied to other plate theories as well, such as the more complete Reissner plate theory whose equilibrium equations were integrated for axisymmetric bending by Hart and Evans[10].

It is well-known that the success of variational solution procedures such as the Ritz method (employed here) is directly dependent on the choice of solution functions. In the present case, realistic stress solutions are due to the use of beam vibration eigenfunctions in the radial dependence of the finite series (11) for the transverse deflection $w(r, \theta)$; in addition to being geometrically admissible, these functions exhibit nonzero derivatives necessary for satisfying natural boundary conditions. Although no natural boundary conditions are imposed here, it is reasonable to expect that bending stresses calculated from functions that *could* satisfy natural boundary conditions should be more accurate than bending stresses calculated from functions that cannot satisfy these conditions. An example is given by the trigonometric functions; these can be geometrically admissible but cannot be simultaneously capable of satisfying natural boundary conditions. The solution of the plate problem presented in this paper was previously attempted by using geometrically admissible trigonometric functions in the transverse displacement series; extremely erratic bending stresses were found.

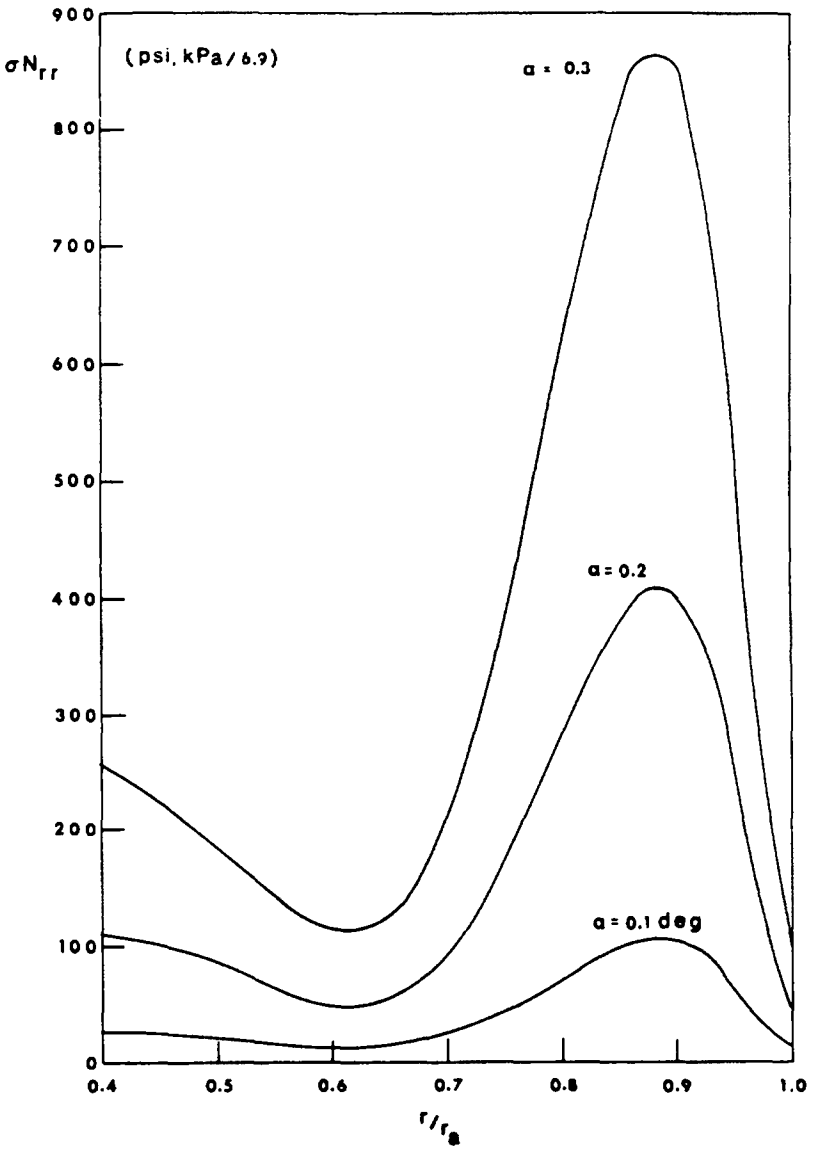

Fig. 9. Influence of a large hub rotation on the membrane stress in a plate with hyperbolic taper.

The application of beam vibration eigenfunctions to obtain approximate solutions of plate and shell problems was apparently first made by Vlasov in a slight variation of Galerkin's method. Vlasov's method is described in the comprehensive book on plates by Szilard[16].

A number of other numerical procedures, including the finite element method[17], have the nonlinear capability necessary to reproduce the solutions presented in the paper. Efficiency, as well as accuracy, is a point to be considered in selecting a solution technique. The efficiency of the energy method as applied here† derives from the use of solution functions that combine into a finite series which closely approximates the exact solution.

Acknowledgements—The major portion of the work described in this paper was sponsored by the Bendix Corporation, Electric and Fluid Power Division.

REFERENCES

1. S. P. Timoshenko and S. Woinowsky-Krieger, *Theory of Plates and Shells*, 2nd Edn. McGraw-Hill, New York (1959).
2. J. E. Brock, Asymmetric moment loading of annular elastic plates. *J. Appl. Mech.* 43, 353 (1976)

†Three Newton-Raphson iterations were the maximum number needed for the solutions shown herein. A complete nonlinear solution, including stress calculations, is obtained in approximately seven seconds of execution time on an Amdahl 470V/6 computer.

3. P. H. W. Wolff, The design of flexible disk misalignment couplings. *Instn Mech. Engrs Appl. Mech. Proc.* **165**, 165 (1951).
4. G. C. Pardoen, Asymmetric bending of circular plates using the finite element method. *Comput. & Struct.* **5**, 197 (1975).
5. G. J. Wilson and J. Kirkhope, Finite element bending analysis of nonuniform circular plates. *Comput. & Struct.* **6**, 459 (1976).
6. W. B. Fraser, Bending of a radially prestressed annular plate by tilting a central rigid inclusion. *J. Elasticity* **5**, 129 (1975).
7. W. E. Alzheimer and R. T. Davis, Unsymmetrical bending of prestressed annular plates. *J. Engng Mech. Div. Am. Soc. Civ. Engrs* **94**, 905 (1968).
8. W. H. Wittrick, Axisymmetrical bending of a highly stretched annular plate. *Q. J. Mech. Appl. Math.* **18**, 11 (1965).
9. J. T. Tielking, Axisymmetric bending of annular plates. *J. Appl. Mech.* **45**, 834 (1978).
10. V. G. Hart and D. J. Evans, Nonlinear bending of an annular plate by transverse edge forces. *J. Math. Phys.* **43**, 275 (1964).
11. W. E. Alzheimer and R. T. Davis, Nonlinear unsymmetrical bending of an annular plate. *J. Appl. Mech.* **35**, 190 (1968).
12. H. L. Langhaar, *Energy Methods in Applied Mechanics*. Wiley, New York (1962).
13. D. Young and R. P. Felgar, *Tables of Characteristic Functions Representing Normal Modes of Vibration of a Beam*. University of Texas Pub. No. 4913 (1949).
14. T. R. Tauchert, *Energy Principles in Structural Mechanics*. McGraw-Hill, New York (1974).
15. W. E. Alzheimer and R. T. Davis, *Unsymmetrical Large Deflections of an Annular Plate*. Virginia Polytechnic Institute Research Division Bulletin No. 9 (1966).
16. R. Szilard, *Theory and Analysis of Plates: Classical and Numerical Methods*, Prentice-Hall, Englewood Cliffs, New Jersey (1974).
17. J. T. Oden, *Finite Elements of Nonlinear Continua*. McGraw-Hill, New York (1972).